Long Haul Time and Frequency Distribution in Different DWDM Systems

Krzysztof Turza, Przemysław Krehlik, and Łukasz Śliwczyński, *Member, IEEE*

***Abstract*— In this paper, we have presented the possibility of time and frequency (T&F) distribution in two generations of dense wavelength-division-multiplexing (DWDM) networks: the older one, equipped with dispersion compensation fiber (DCF) modules, and the newest, without in-line chromatic dispersion compensation (dedicated for coherent signals). The experiments were performed in a 1500-km loop arranged in the PIONIER production network, with T&F signals regarded as so-called "alien wavelength" network service. In the newest DWDM version, we observed very good stability of delivered signals: modified Allan deviation approach 10^{-16} for averaging longer than 10^4 s (for 10-MHz frequency signal), and time deviation below 15 ps for averaging up to 10^5 s for 1 PPS time signal. These results show that the DWDM alien wavelength service can be used for high-demanding applications like cesium fountains comparisons. Results achieved for the former version of DWDM were about one magnitude worse for a long-term comparison, but it can still be useful for less demanding applications. We found that the main reason for relatively poor results observed in the older generation of DWDM is the impact of the DCFs used in this DWDM approach.**

***Index Terms*— Alien wavelength, dense wavelength-division-multiplexing (DWDM) network, optical fiber, time and frequency (T&F) transfer.**

I. INTRODUCTION

IN THE past few years, a number of projects have exploited possibilities of the time and frequency (T&F) signals transfer based on dedicated fiber (dark fiber) or channel [1]–[6]. These proved that the use of optical fibers can offer a new quality in accurate comparison and distribution of T&F sources.

An optical fiber, as any transmission medium, displays some fluctuations of the propagation delay, caused by environmental factors. The main source of fluctuations (noise) is the impact of temperature, which affects both the physical length of the fiber and the refractive index of the silica glass. Moreover, so-called acoustic noise caused by variable strains (vibrations) modulates the fiber length, and thus the output signal phase [7]–[9]. Various ideas for reducing the propagation instability [10]–[14] are based on redirecting the signal reaching the remote end of the link backward to the local side, and arranging a feedback system which can compensate the fluctuations of the phase (or delay) of propagating signals. The underlying idea of all these solutions is to use the single optical fiber bidirectionally, to gain from (nearly) perfect correlation of fiber-related noise in forward and backward directions.

However, renting dedicated fibers especially for long distance connections, is very costly or sometimes even impossible. In this situation, some alternative methods are desired, even sacrificing the performance to some reasonable extent. One of possible solutions is to perform a deep hardware modification in a standard telecommunication optical network, to allow bidirectional signal transmission in a fiber basically intended for unidirectional usage [4], [15]. The other solution, investigated herein, is the concept of using a unidirectional dedicated channel in a currently used telecommunication dense wavelength-division-multiplexing (DWDM) network, in combination with well-tested endpoints dedicated for "dark fiber." Modern telecommunication networks allow to inject an alien, optical signal from external devices (so-called alien wavelength), and transmit it through the network without electrical regeneration [16], [17].

Unfortunately, when using a DWDM channel for T&F transfer, the forward–backward symmetry is deteriorated because there are physically different optical paths for both directions [10], [18], [19]. The impact of this asymmetry on T&F transfer would be twofold; unequal propagation delay for forward and backward paths affects accuracy of time transfer calibration, and unequal delay fluctuation affects the effectiveness of any active delay stabilizing system, thus worsening transfer stability [20]. Analyzing the sources of asymmetry, two main areas may be pointed out. The first area is related to the optical cables connecting the network nodes. As the fibers used for forward and backward transmission are located in the same cable, the impact of environmental temperature seems to be highly correlated. However, the acoustic noise related to very local tensions, vibrations, and frictions affecting the fibers, could be less correlated. The second type area of asymmetry is related to network nodes, performing various processing of the optical signal, as amplification, optical routing, filtering, and dispersion compensation. It should be stressed that this processing is done not only in two physically different paths but might be desirably and substantially different for forward and backward signals. For instance, a commonly used strategy of optical amplification and dispersion compensation leads to nonsymmetric treatment of opposite directions in particular nodes.

All the experiments presented herein were performed with the ELSTAB devices [21] originally developed for the

---

Manuscript received January 18, 2018; accepted April 11, 2018. Date of publication April 17, 2018; date of current version June 26, 2018. This work was supported in part by the OFTEN 15SIB05 Project. The OFTEN Project was supported by the EMPIR programme co-financed by the Participating States and by the European Union's Horizon 2020 Research and Innovation Programme. *(Corresponding author: Krzysztof Turza.)*

K. Turza is with the Network Technology Division, Poznań Supercomputing and Networking Center, Polish Academy of Science, 61-139 Poznań, Poland (e-mail: kturza@man.poznan.pl).

P. Krehlik and Ł. Śliwczyński are with the Faculty of Computer Science, Electronics, and Telecommunications, AGH University of Science and Technology, 30-059 Krakow, Poland (e-mail: krehlik@agh.edu.pl).

Digital Object Identifier 10.1109/TUFFC.2018.2827178

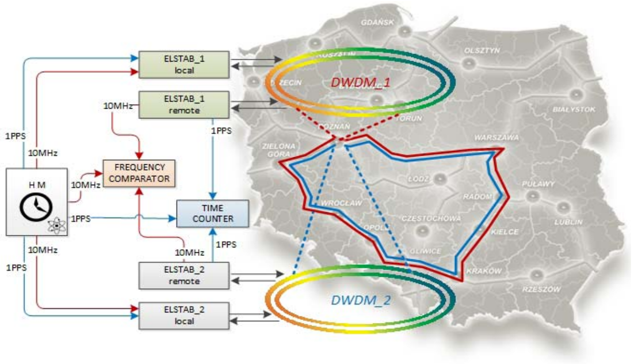

Fig. 1. Block diagram for experimental frequency transfer.

bidirectional dark fiber approach, but, here, adopted for the alien wavelength service in the DWDM network. The measurements were made in a fully production PIONIER telecommunication network (the National Research and Education Network in Poland) operated by Poznan Supercomputing and Networking Center. In particular, we extend our investigations to the modern DWDM networks that have appeared with the advent of coherent 100-Gb/s technology. The essential feature of such a network is that the use of spooled dispersion compensating fibers that substantially increase the asymmetry of the link is completely abandoned. Thus, better results comparing to standard DWDM networks (dedicated for 10-Gb/s signals) can be expected.

II. Testbed Architecture

The main experiments were arranged within the PIONIER network in the form of two parallel 1500-km long loops (Fig. 1), running on separate fibers of the same underground cable. The first loop (hereafter referred as DWDM_1) carries a number of noncoherent 10-Gb/s signals and exploits dispersion compensation fiber (DCF) modules. The next one (hereafter referred to as DWDM_2) is designed for transport of coherent optical signals (during the tests, there were several 100-Gb/s transmissions) and it has no inline DCF modules at all. Both loops use advanced reconfigurable add drop multiplexer (ROADM) modules for optical wavelength routing. All DWDM components were FSP3000 series devices made by ADVA Optical Networking.

T&F signals (1 PPS and 10 MHz) from a passive hydrogen maser were connected to AGH-developed ELSTAB local and remote units which fed their optical signals directly into the DWDM systems. Both ends of ELSTAB (local and remote) were located at the same laboratory. Block diagram of the setup exploited in the experiments is shown in Fig. 1.

The ELSTAB units were adapted to the unidirectional transmission over the pair of fibers in a single (50-GHz spacing) DWDM channel. The stability of the frequency transfer was assessed in both parallel DWDM_1 and DWDM_2 loops at the same time by measuring the residual phase fluctuations between the input reference signal (10-MHz frequency supplied to ELSTAB local units) and the output signal from the remote units using a dual-channel VCH-314 phase comparator (Vremya-CH). The measurements gave us an overview of the efficiency of the delay compensation in these two different DWDM solutions. The stability of 1 PPS signal was measured by the multichannel, picosecond-resolution time interval counter MTC-108 [22] (developed by the Polish Military University of Technology, Warsaw, Poland).

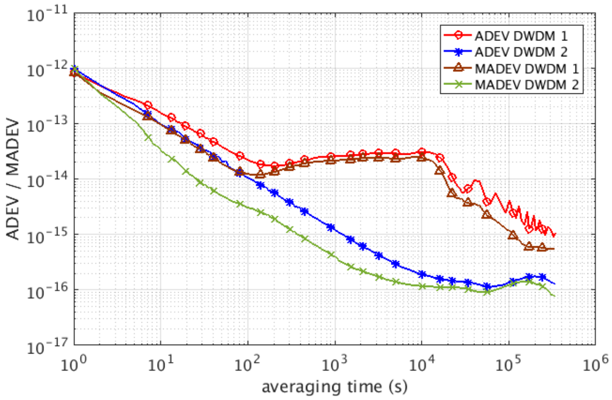

Fig. 2. ADEV and MADEV in DWDM_1 type and DWDM_2.

III. Measurement Results

The analysis of measurements presented below is divided into two sections. Section III-A presents the frequency transfer (10 MHz) evaluated in two different types of DWDM networks. Section III-B concentrates mostly on the possibility of transfer of the calibrated time (1 PPS) using a DWDM channel approach.

A. Frequency Transfer Stability

The following analysis presents the capability of the transmission of 10-MHz signal in DWDM_1 and DWDM_2 networks. By performing simultaneous frequency transfer (under the same external conditions) in two systems operating in parallel, we were able to reliably compare them and also to make much more precise analysis and identification of possible sources of the transfer instability.

1) Comparison of the Frequency Transfer in Two Types of DWDM Networks: The measurements of phase changes of 10-MHz signals transmitted with ELSTAB units were performed during the observation period lasting for over 20 days. Fig. 2 shows the plots of a fractional frequency stability calculated from the measured data.

The green line [modified Allan deviation (MADEV) measured in DWDM_2] shows that the white phase modulation (PM) and next flicker PM noises play a major role up to 2000 s of the average time. It gives fast averaging improvement and after 3 h it achieves the stability at the level of 1.2×10^{-16}. For longer averaging times, the flicker frequency modulation (FM) noise starts to play a major role.

The brown line (MADEV measured in DWDM_1) shows the slope of τ^{-1} only for averaging times lower than about 100 s. After that, the curve is possibly dominated by a flicker FM noise and oscillating noises. For this middle term averaging time ($100 < \tau < 15\,000$ s), the stability does not exceed 1.2×10^{-14}. Longer averaging brings some improvement of stability that approaches 6×10^{-16}.

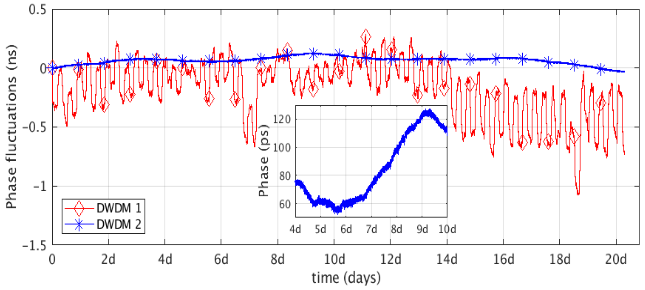

Fig. 3. Residual phase fluctuations of the 10-MHz signal in DWDM_1 and DWDM_2 systems. Inset: enlarged part of trace for DWDM_2.

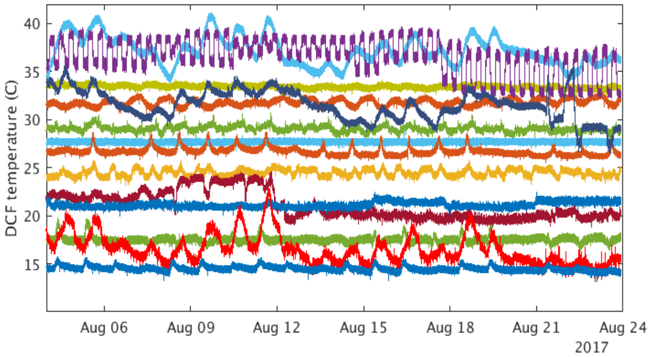

Fig. 4. Temperatures of DCF components collected across the line (some of traces shifted vertically to avoid overlapping).

Such huge observed difference in the stability of the frequency transfer in different DWDM networks encouraged us to make in-depth investigations. To do so, we looked closely at the phase fluctuations in the time domain.

Fig. 3 presents the residual phase fluctuations of the 10-MHz signal, transmitted over DWDM_1 and DWDM_2. The oscillating character that is evident in residual phase fluctuations in DWDM_1 is quite interesting. These quite stable periodic oscillations with period of about 8 h could not be caused by outside conditions (weather and temperature) because both DWDM_1 and DWDM_2 used the same fiber infrastructure (fibers running inside the same cables). This means that all distortions caused by line cables should have very similar impact on both systems. Thus, the source of such periodic oscillations should be attributed to network nodes (the DWDM equipment and their environment). To find some hint on the origin of this observation, we analyzed the temperature data from all network nodes along the optical path.

2) Temperature Impact: We gathered the temperature data from more than 60 sensors located in various devices in the network nodes. The sensors were factory mounted directly on the individual DWDM modules and the temperature data were stored every 10 s. We paid special attention to devices that make DWDM_1 different from DWDM_2, in particular DCFs (see Fig. 4 for some illustrative examples).

Having analyzed the data from all network nodes, we found one node where the temperature changes (the purple curve in Fig. 4) correlate very well with residual, uncompensated phase changes of transmitted 10-MHz signal in DWDM_1 (see Fig. 5). It was interesting that this particular point of the network had such a significant impact on the DWDM_1 transmission itself, but it was not visible on DWDM_2, despite the fact that both the systems have devices placed at this location. In addition, similar or larger temperature variations in other nodes did not cause such large phase noise. Closer analysis showed that the reason for such a high phase fluctuations is substantial inequality of the lengths of DCF modules in the forward and backward directions in this particular node—see also equation (1).

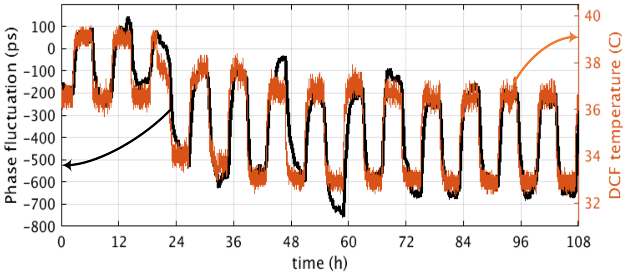

Fig. 5. Measured residual phase fluctuations in DWDM_1 and its correlation with the changes of DCF's temperature in the most significant node.

Based on the vendor's data, we estimated the length of the forward direction DCF (L_{DCF}) as 5 and 10 km for the backward direction, respectively. Assuming fiber propagation delay thermal coefficient (denoted as A in following equation) of 38 ps/(km·K) [23], [24], and taking into account that a half of the forward–backward propagation asymmetry is visible at the output of the delay stabilizing system [21], one could calculate the impact of this DCFs temperature (T) fluctuations as 95 ps/K, which agrees very well with the measurement data visible in Fig. 5.

For further investigation of the impact of DCFs on T&F transfer stability in DWDM_1, we calculated the cumulated impact of all involved DCF spools in our link by using the following equation. We added up the contributions from all DCFs, taking with "+" sign the forward DCFs, and with "−" the backward ones (marked with a "prime" sign)

$$\Delta\tau = \frac{1}{2} A \sum_{i=1}^{n} \left(L_{\mathrm{DCF}_i} \cdot \Delta T_{\mathrm{DCF}_i} - L'_{\mathrm{DCF}_i} \cdot \Delta T'_{\mathrm{DCF}_i} \right). \quad (1)$$

Using the temperature data registered for all DCFs, we calculated the hypothetical delay fluctuations at the output of the T&F transfer system, and compared the resulting MADEV with that actually measured (see Fig. 6). For averaging periods longer than about 1 h, we observed nearly perfect agreement between the anticipated impact of DCFs and measured results, which let us conclude that temperature fluctuations affecting the DCF modules used in DWDM_1 system clearly dominate the overall long-term stability of T&F transfer in such type of network. Unfortunately, for averaging shorter than 1 h, our prediction strongly overestimates the real instability, because the noise of the entire ensemble of sensors builds up unrealistically high short-term noise in our "hypothetical" phase fluctuations (over 200-ps rms instead of 10-ps rms for 100-s averaging).

In DWDM links equipped with DCFs modules, the actual range of phase changes and its frequency spectrum will be

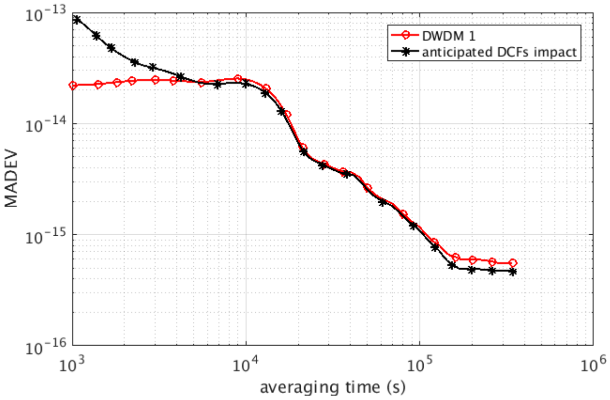

Fig. 6. MADEV analysis in DWDM_1 in context of DCF's temperature fluctuations.

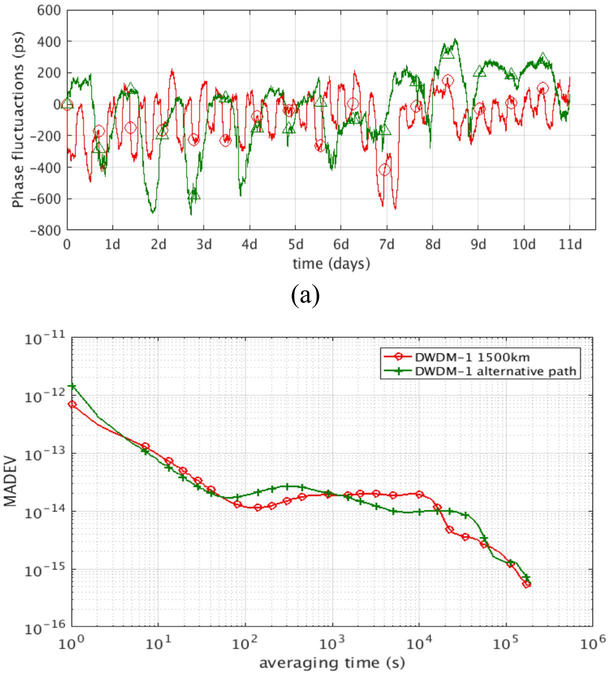

(a)

(b)

Fig. 7. (a) Phase fluctuations and (b) MADEV of 10-MHz signal in DWDM_1 system on two different paths.

different on each line. They will be strictly dependent on combination of DCF configuration and their temperature changes. Fig. 7(a) shows the comparison of 10-MHz frequency stability measurements in our primary path (presented in Section II) and in a different route (800-km loop) but at the same kind of DWDM_1 system. Fluctuations of different shapes and periods can be observed in these two cases, probably because of different temperature conditions in the particular network nodes. But despite of this, MADEV [Fig. 7(b)] is generally quite similar in both cases: for medium averaging periods (from 100 s until about half a day), stability of frequency transfer is close to 1×10^{-14}, and only very long averaging can give better stability, approaching 1×10^{-15}.

Summarizing the above considerations, it should be noted that the use of DCFs in DWDM systems severely affects the stability of frequency transfer. Basically, the impact of DCFs could be lowered if they were installed symmetrically in the line (i.e., the same values for both directions at each node). Unfortunately, in typical telecommunication systems, location of DCF modules is optimized to achieve minimal losses (to lower the number of amplifiers) and maximize the optical signal-to-noise ratio. It is common that modules with different values in both directions can be found in one node.

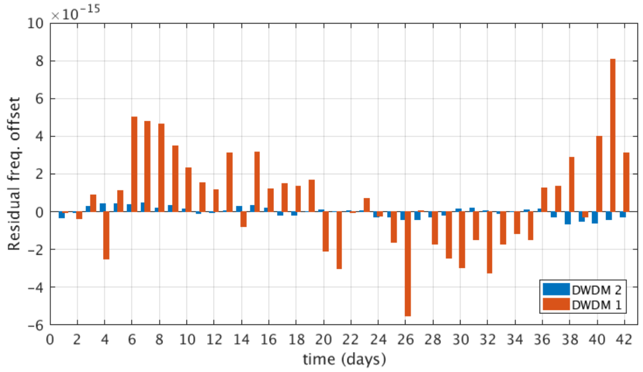

Fig. 8. Residual frequency offset (daily averaged) in DWDM_1 and DWDM_2 systems.

3) Frequency Offset: For a comprehensive illustration of the long-term accuracy of frequency transfer in DWDM systems, a daily averaged, residual frequency offset was also analyzed. Fig. 8 shows the results for both DWDM_1 and DWDM_2.

As it can be seen on the graph (Fig. 8), the transmission in DWDM_1 system is burdened with a fairly large offset. In the analyzed period of time, the daily averaged frequency error ranged from -5.5×10^{-15} to $+8 \times 10^{-15}$, and its root mean square value in DWDM_1 is 2.7×10^{-15}. For DWDM_2 transmission, the daily averaged frequency offset is approximately an order of magnitude lower, ranging from -6.4×10^{-16} to 4.8×10^{-16}, and its root mean square value is 2.9×10^{-16}. Estimated uncertainty of this daily averaged measurements performed with VCH-314 phase comparator is 0.8×10^{-16}. The frequency offset averaged over entire 42-days period was 6.1×10^{-16} for DWDM_1 and 2.5×10^{-17} for DWDM_2.

B. Time Transfer Capability

The following analysis shows the transmission capabilities of 1 PPS signals in two types of DWDM networks. Similar to all time transmissions based on a pair of fibers, it is impossible to precalculate the absolute line delay due to the differences in forward and backward directions. It should be noted that in all similar cases, precalibration done by an external, reference time transfer system is necessary [exploiting, e.g., Global Navigation Satellite Systems (GNSS) data]. An asymmetry analysis in DWDMs systems and stability of time transfer based on the measurements made in our testbed are presented below.

1) Time Transfer Asymmetry: The unidirectional transmission does not have perfect optical length symmetry in forward and backward directions, which seriously affected the time transfer calibration. The main part of this asymmetry is imposed by DWDM nodes. Individual modules for each direction have different positions in the rack, which results in different lengths of patchords. Moreover, each

TABLE I

ASYMMETRY IN VARIOUS DWDM'S LOOPS

DWDM TYPE	1	1	**1**	**2**	2
DCFs modules	YES	YES	**YES**	**NO**	NO
Link length [km]	797	1770	**1534**	**1534**	2177
Asymmetry [ns]	–2586	–9784	**+3930**	**+144**	+69
Estimated asymmetry [m] *	–529	–2001	**+804**	**+29**	+14

* *The asymmetry has been estimated based on time-domain asymmetry*

amplifiers [erbium-doped fiber amplifiers (EDFAs)], chromatic dispersion compensation modules (DCFs) and other DWDM's components do not have the same optical length. The next source of asymmetry are the line fibers. Even though these fibers are at the same cable, their length is not exactly the same in both directions due to production and splicing technology. All these aspects can cause various asymmetry values in different particular cases. We made asymmetry measurements on five routes (three in DWDM type 1 and two in the DWDM type 2), configured in loop topology in the PIONIER network. We used a standard procedure for ELSTAB time transfer calibration, developed for bidirectional, one-fiber link [21] to anticipate the 1 PPS delay at the remote module output. The actually measured delays were seriously different, which was attributed to the two-fiber-based link asymmetry, and gives an insight into time transfer calibration uncertainty in DWDM networks. The results are presented in Table I.

Sign "+" in asymmetry means that the backward line is shorter than the forward one and "–" means the opposite situation. In the above analysis, a very large difference in asymmetry between the two types of DWDMs is noted. Total asymmetry in the 1500-km DWDM_2 loop (without DCFs) was 144 ns, which is equivalent to 30 m of fiber. At the same route the DWDM_1 asymmetry was over 27 times bigger. These values obtained for DWDM_1 are similar to those presented in [25], where the same kind of DWDM networks were used. In this kind of DWDM networks (type 1), the major role is played by large spread of each DCF modules length.

The data presented in Table I shows that the optical path asymmetry in DWDM type 2 is at the level of several hundred nanoseconds but in DWDM type 1 (with DCFs modules) it is a few microseconds. Thus, an initial calibration for time (1 PPS) transfer based on some external means is necessary in both kinds of DWDM networks. Moreover, this calibration has to be repeated after each optical fiber failure or intentional physical path change. Practically, in typical European conditions, a mean time between failures for a long-haul link may be estimated in the rage from several months up to more than a year.

2) Impact of the Transmission in DWDMs on the Time Deviation and Maximum Time Interval Error: The results of the over 20 days measurement session are shown in Fig. 9, presenting the time deviation (TDEV) of 1 PPS pulses transfer in DWDM types 1 and 2 (in the over 1500-km loop).The reference signals from the hydrogen maser (input signals to ELSTAB units) were compared with 1 PPS signals in the output of remote units. These signals were measured by time interval counter (MTC-108).

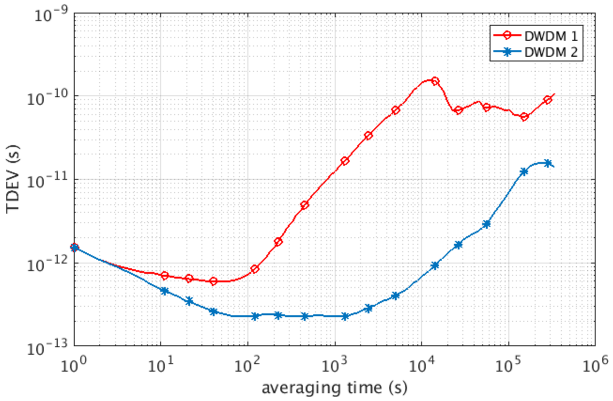

Fig. 9. TDEV of 1 PPS signals in DWDM 1 and 2.

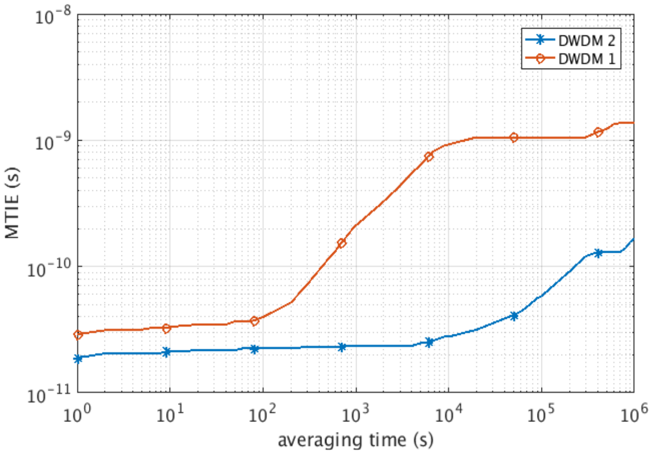

Fig. 10. MTIE in the DWDM_1 and DWDM_2 transmission.

For the transmission in DWDM_1, and the averaging times greater than 10 s, the value of TDEV is below 0.7 ps, reaching its minimum around 0.6 ps near 50 s. For the averaging period higher than 100 s, the flicker FM noise starts to dominate and degrade the TDEV up to 150 ps. This is the worst value corresponding with a half of period of uncompensated oscillating noise (4 h). Longer averaging gives time transfer stability near 100 ps.

The time transfer in DWDM_2 gives much better stability results. For the averaging greater than 50 s the value of TDEV is below 250 fs and it is 350 fs better than in DWDM_1. The TDEV of transmission in DWDM_2 reaches its minimum around 230 fs near 80 s. The longer averaging (up to 1500 s) does not provide any improvements in stability. For τ longer than 1500-s, noise degraded the stability up to 15 ps (near two days observation). In case of very long averaging, stability in DWDM_2 is around one order of magnitude better than in DWDM type 1.

Fig. 10 presents the maximum time interval error (MTIE) of 1 PPS transmission in DWDMs (calculated from the same data

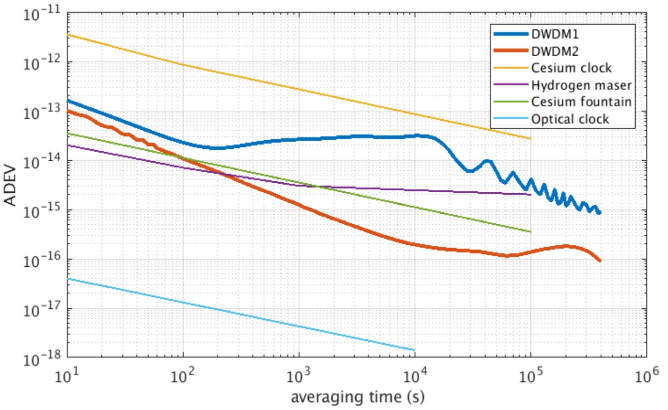

Fig. 11. Frequency performance transmitted in DWDM shown in the background of various atomic frequency standards.

as used for TDEV). The lowest error introduced by transmission in DWDM_1 is only for a short averaging window up to 100 s. In this range, error does not exceed 35 ps. For longer averaging time, MTIE rises to about 1 ns. DWDM_2 gives much better results. For averaging time up to 2.5 h, MTIE is about 20 ps. The length of the period with very good accuracy is much longer than it was in the DWDM_1. Long term averaging gives MTIE of about 150 ps, and it is almost one order of magnitude better than it was in DWDM_1.

IV. DISCUSSION OF RESULTS

The stability of frequency transmission in DWDM systems in relation to the stability of various clocks is presented on Fig. 11. The DWDM_1 system can be used to distribute the frequency signal with stability not worse than the currently used cesium clocks [26]. This can be a reasonable solution for less demanding users who need stability in the range of a few times 10^{-14}, and are not prepared for maintaining and controlling their own clocks.

A much wider range of applications is possible using frequency transfer in the DWDM_2 system. Its stability above 100 s of averaging time is comparable even with cesium fountains [27]. It will also enable the distribution and comparison of frequencies generated by active hydrogen masers [28] without significant stability degradation.

It should be emphasized that the effect of link asymmetry and, as a result, residual delay fluctuations have their impact on the frequency offset (Section III-A3). The long-haul frequency transfer in the DWDM_2 can be suitable for clocks comparison with frequency uncertainty at the level of the few 1×10^{-16}. It can be useful even for the preliminary optical clocks evaluation [29], [30].

In comparison to commonly used GNSS transmission methods, such as common view or precise point positioning [31], [32], the DWDM_2-based transfer offers approximately an order of magnitude better stability (in the whole averaging time range). The DWDM_1 system is comparable to GNSS methods or slightly less stable in the averaging range from 10^3 to 10^5 s, but for longer integration time can give better results. However, it should be emphasized that the systems presented in this paper can be used for on-line distribution of T&F signals, in contrast to satellite methods which are useful only for off-line comparison of the distant clocks.

Our experiments proved that for the users who need quite a stable and accurate frequency, the transfer using the DWDM approach is an interesting approach to choose. Using this, a new service "frequency on demand" should be possible. The idea is to dynamically establish a link on demand between the signal source (for example the ELSTAB local unit connected to high-accuracy frequency standard) and any remote unit through a DWDM system. The widely used optical switching modules (ROADMs) enable a flexible and fully optical setup of such a service in modern DWDM networks, through the operator and a dedicated management system (including the latest solutions—Software Define Networks [33]). Also the long-haul version of ELSTAB units (used in our testbed) support fully automated adjustment to new line conditions (auto adjust to the any line delay changes). This solution could be particularly useful for periodic dissemination of the high-accuracy frequency source to end users and for dedicated device calibration/comparison sessions.

In case of time transfer in DWDM, there is a problem of absolute time calibration. It must be implemented using external systems (GNSS or using self-calibrating bidirectional fiber optic systems [1], [25]). In addition, this calibration must be performed after any failure or reconstruction of the DWDM system. However, T&F transfer systems based on DWDM can be successfully used as backup systems. Once calibrated, such a link is a very good reference until the next network failure/reconstruction. It gives the possibility of very accurate real-time comparisons of time sources, detection of potential attacks, and breakdowns of the GNSS network (it largely makes the user independent of satellite systems). The link based on DWDM, mainly due to its moderate cost, can be a very good backup solution for the "dark fiber" solutions, and thus, guarantee the continuity of service provision in the event of a failure of the primary link.

V. CONCLUSION

It has been demonstrated that the DWDM network construction strongly influences the stability of T&F signal transmission. In particular, chromatic dispersion compensators (DCFs) and their placement along the line have a very significant influence on the transmission quality. The results of transmission in the newest DWDM systems architecture, dedicated for coherent transmission, are surprisingly good. Allan deviation of frequency transfer in this solution approach 10^{-16} for averaging longer than 10^4 s, and TDEV is below 15 ps. This gives hope for widespread use of this type of DWDM in the T&F distribution. The former version of DWDMs with DCF spools is still commonly used and its stability, about an order of magnitude worse than in the newer one, can still be in the scope of a slightly less demanding application.

REFERENCES

[1] L. Śliwczyński, P. Krehlik, A. Czubla, L. Buczek, and M. Lipiński, "Dissemination of time and RF frequency via a stabilized fibre optic link over a distance of 420 km," *Metrologia*, vol. 50, no. 2, pp. 133–145, Feb. 2013.

[2] L. Buczek *et al.*, "OPTIME-the system grows—A new 330 km line," in *Proc. Joint Conf. IEEE Int. Freq. Control Symp. Eur. Freq. Time Forum*, Denver, CO, USA, Apr. 2015, pp. 583–586.

[3] V. Smotlacha and A. Kuna, "Two-way optical time and frequency transfer between IPE and BEV," in *Proc. Eur. Freq. Time Forum (EFTF)*, Gothenburg, Sweden, Apr. 2012, pp. 375–378.

[4] J. Vojtech, V. Smotlacha, and P. Skoda, "Simultaneous transmission of accurate time in parallel with stable optical frequency in real fibre network over 612 km," in *Proc. Optoelectron. Global Conf. (OGC)*, Shenzhen, China, Aug. 2015, pp. 1–3.

[5] X. Chen *et al.*, "Simultaneously precise frequency transfer and time synchronization using feed-forward compensation technique via 120 km fiber link," *Sci. Rep.*, vol. 5, Dec. 2015, Art no. 18343.

[6] J. Guéna *et al.*, "First international comparison of fountain primary frequency standards via a long distance optical fiber link," *Metrologia*, vol. 54, no. 3, p. 348, May 2017.

[7] L. G. Cohen and J. W. Fleming, "Effect of temperature on transmission in lightguides," *Bell Syst. Tech. J.*, vol. 58, no. 4, pp. 945–951, Apr. 1979.

[8] C. N. Pannell, J. D. C. Jones, and D. A. Jackson, "The effect of environmental acoustic noise on optical fibre based velocity and vibration sensor systems," *Meas. Sci. Technol.*, vol. 5, no. 4, p. 412, 1994.

[9] Ł. Śliwczynski and P. Krehlik, "Measurement of acoustic noise in field-deployed fiber optic cables," in *Proc. Eur. Freq. Time Forum (EFTF)*, Neuchatel, Switzerland, Jun. 2014, pp. 339–342.

[10] P. A. Williams, W. C. Swann, and N. R. Newbury, "High-stability transfer of an optical frequency over long fiber-optic links," *J. Opt. Soc. Amer. B, Opt. Phys.*, vol. 25, no. 8, pp. 1284–1293, Aug. 2008.

[11] L. Primas, G. Lutes, and R. Sydnor, "Fiber optic frequency transfer link," in *Proc. 42nd Annu. Freq. Control Symp.*, Jun. 1988, pp. 478–484.

[12] D. Johnson, M. Calhoun, R. Sydnor, and G. Lutes, "A wide-band fiber optic frequency distribution system employing thermally controlled phase compensation," in *Proc. 24th Annu. Precise Time Time Interval (PTTI) Meeting*, Jun. 1993, pp. 365–374.

[13] C. E. Calosso *et al.*, "Frequency transfer via a two-way optical phase comparison on a multiplexed fiber network," *Opt. Lett.*, vol. 39, no. 5, pp. 1177–1180, 2014.

[14] Ł. Śliwczynski, P. Krehlik, Ł. Buczek, and M. Lipiński, "Active propagation delay stabilization for fiber-optic frequency distribution using controlled electronic delay lines," *IEEE Trans. Instrum. Meas.*, vol. 60, no. 4, pp. 1480–1488, Apr. 2011.

[15] F. Kéfélian, O. Lopez, H. Jiang, C. Chardonnet, A. Amy-Klein, and G. Santarelli, "High-resolution optical frequency dissemination on a telecommunications network with data traffic," *Opt. Lett.*, vol. 34, no. 10, pp. 1573–1575, May 2009.

[16] A. Colmenero *et al.* (Jul. 2016). *Deliverable D13.2 Blueprint of Services and Research Plan for Future Work*. [Online]. Available: https://www.geant.org/Projects/GEANT_Project_GN4-1/Documents/D13-2_Blueprint-of-Services-and-Research-Plan-for-Future-Work.pdf

[17] A. Lord, P. Wright, and Y. R. Zhou, "Alien waves: Technology, benefits and standardisation," in *Proc. Int. Conf. Photon. Switching (PS)*, Ajaccio, France, Sep. 2012, pp. 1–3.

[18] Ł. Śliwczyński, P. Krehlik, M. Lipiňski, K. Turza, and A. Binczewski, "Frequency distribution in delay-stabilized optical DWDM network over the distance of 3000 km," in *Proc. Joint Conf. IEEE Int. Freq. Control Symp. Eur. Freq. Time Forum*, Denver, CO, USA, Apr. 2015, pp. 280–283.

[19] C. Daussy *et al.*, "Long-distance frequency dissemination with a resolution of 10^{-17}," *Phys. Rev. Lett.*, vol. 94, nos. 20–27, p. 203904, 2005.

[20] A. Bercy, F. Stefani, O. Lopez, C. Chardonnet, P.-E. Pottie, and A. Amy-Klein, "Two-way optical frequency comparisons at 5×10^{-21} relative stability over 100-km telecommunication network fibers," *Phys. Rev. A, Gen. Phys.*, vol. 90, p. 061802, Dec. 2014.

[21] P. Krehlik, L. Śliwczyński, Ł. Buczek, J. Kołodziej, and M. Lipiński, "ELSTAB—Fiber-optic time and frequency distribution technology: A general characterization and fundamental limits," *IEEE Trans. Ultrason., Ferroelectr., Freq. Control*, vol. 63, no. 7, pp. 993–1004, Jul. 2016.

[22] D. Sondej, M. Sawicki, and R. Szplet, "An autonomous microcontroller system for controlling a multi-channel time counter," *Meas. Autom. Monitor.*, vol. 61, no. 7, pp. 305–307, Jul. 2015.

[23] K. T. V. Grattan, and B. T. Meggitt, *Optical Fiber Sensor Technology*. Dordrecht, The Netherlands: Kluwer, 1999, p. 115.

[24] Ł. Śliwczyński, P. Krehlik, and M. Lipiński, "Optical fibers in time and frequency transfer," *Meas. Sci. Technol.*, vol. 21, no. 7, p. 075302, May 2010.

[25] E. F. Dierikx *et al.*, "White rabbit precision time protocol on long-distance fiber links," *IEEE Trans. Ultrason., Ferroelectr., Freq. Control*, vol. 63, no. 7, pp. 945–952, Jul. 2016.

[26] *The Specification of Cesium Clock 5071A*. Accessed: Jan. 2018. [Online]. Available: https://www.microsemi.com/product-directory/cesium-frequency-references/4115-5071a-cesium-primary-frequency-standard

[27] C. Tamm *et al.*, "CS-based optical frequency measurement using cross-linked optical and microwave oscillators," *Phys. Rev. A, Gen. Phys.*, vol. 89, p. 023820, Feb. 2014.

[28] *The Specification of Active Hydrogen Maser VCH-1003A*. Accessed: Jan. 2018. [Online]. Available: http://www.vremya-ch.com/english/product/index.html

[29] M. Schioppo *et al.*, "Ultrastable optical clock with two cold-atom ensembles," *Nature Photon.*, vol. 11, pp. 48–52, Jan. 2017.

[30] I. Ushijima, M. Takamoto, M. Das, T. Ohkubo, and H. Katori, "Cryogenic optical lattice clocks," *Nature Photon.*, vol. 9, pp. 185–189, Feb. 2015.

[31] P. Defraigne and Q. Baire, "Combining GPS and GLONASS for time and frequency transfer," *Adv. Space Res.*, vol. 47, no. 2, pp. 265–275, Jan. 2011.

[32] J. Delporte and F. Mercier, "Recent improvements in GPS carrier phase frequency transfer," in *Proc. IEEE Int. Freq. Control Symp. Expo.*, Aug. 2005, pp. 699–706.

[33] A. L. Soso, G. Bruno, and J. Nijhof, "DWDM optical extension to the transport SDN controller," in *Proc. Fotonica AEIT Italian Conf. Photon. Technol.*, Turin, Italy, May 2015, pp. 1–4.

Krzysztof Turza received the M.Sc. degree in electronics and telecommunication science from the Poznan University of Technology, Poznań, Poland, in 2004.

Since 2004, he has been with the Network Department of Poznan Supercomputing and Networking Center, Poznań, where he is responsible for the operation and maintenance of the PIONIER network as a Network Specialist. His research and development activities have been concentrated on T&F transfer systems based on DWDM and dedicated fiber infrastructure.

Przemysław Krehlik received the M.Sc. and Ph.D. degrees in electronics from the AGH University of Science and Technology, Krakow, Poland, in 1988 and 1998, respectively.

Since 1988, he has been with the Fiber Optic Transmission Group, Department of Electronics, AGH University of Science and Technology. He has authored or co-authored more than 60 papers in journals and conference proceedings. His research and development activities include electronic circuits, direct modulation of semiconductor lasers, and application-specific fiber-optic systems.

Łukasz Śliwczyński (M'13) received the M.Sc. and Ph.D. degrees from the AGH University of Science and Technology, Krakow, Poland, in 1993 and 2001, respectively.

He has authored or co-authored more than 60 papers in journals and conference proceedings. He has worked on various high-speed transmitters and receivers for digital fiber optic transmission systems, and precise T&F transfer systems exploiting optical fibers.